ISSN 0023-1584, Kinetics and Catalysis, 2006, Vol. 47, No. 2, pp. 213–220. © MAIK "Nauka/Interperiodica" (Russia), 2006.
Published in Russian in Kinetika i Kataliz, 2006, Vol. 47, No. 2, pp. 215–222.

Ion Pairs Formed in Metallocene-Based Systems by the "Double Activation" Mechanism and Their Catalytic Activity[1]

L. Yu. Ustynyuk[a], E. A. Fushman[b], and A. Razavi[c]

[a] *Faculty of Chemistry, Moscow State University, Moscow, 117234 Russia*

[b] *Semenov Institute of Chemical Physics, Russian Academy of Sciences, Moscow, 117977 Russia*

e-mail: elga@polymer.chph.ras.ru

[c] *Centre de Recherche Du Groupe Total, Zone Industrielle C, B-7181 Seneffe (Feluy), Belgium*

Received August 8, 2005

Abstract—The DFT method is used to study the interaction between metallocene catalyst precursors used in ethylene and propylene polymerization and two molecules of the Al-containing cocatalyst $Al(C_6F_5)_3$. The participation of two Al centers in metallocene activation accounts for the catalytic activity and other properties of the catalytic systems. Two energy parameters characterizing the number of active sites and the polymerization rate per site are calculated.

DOI: 10.1134/S0023158406020091

There are two kinds of effective activators for homogeneous metallocene-based systems. The first kind is tris(perfluorophenyl)boron compounds. With these activators, polymerization occurs readily at an equimolar ratio of components [1, 2]. The species formed by metallocenes and these activators fit the modern concepts of the active polymerization site. In particular, considerable charge separation takes place and one of the ligands (an alkyl group) is almost completely shifted towards boron. Such ion pairs were studied by X-ray crystallography [1]. The mechanism of their interaction with olefin molecules was thoroughly studied in a number of theoretical works [3–5].

MAO is the most widely used commercial cocatalyst. With this activator, a rather large molar ratio of aluminum to transition metal (M) is required for efficient polymerization. What is responsible for the unique cocatalyst properties of MAO? What is the structure of the Al-containing counterion? These questions are still to be answered.

Tris(perfluorophenyl)aluminum, another aluminum-containing activator, has recently become popular [6, 7]. Systems with this activator are not active in polymerization at equimolar ratios of Al to M [6]. Like MAO-containing systems, they become active in propylene and diene polymerization only at larger Al : M ratios.

Chen et al. [6] and Eilertsen et al. [8] suggested a mechanism based on the "double activation" of metallocenes for the formation of catalytic sites in olefin polymerization. According to this mechanism, the catalytic complex adduct contains a metallocene molecule and two Al-containing molecules.

Chen et al. [6] isolated and characterized, by X-ray crystallography, a complex of SBI–$ZrMe_2$ with two $Al(C_6F_5)_3$ molecules, namely, *rac*-$Me_2Si(\eta^5\text{-}Ind)_2Zr[Me\text{–}Al(C_6F_5)_3]_2$. They also suggested the formation of the ion pair $[\{L\}MMe]^+[(C_6F_5)_3Al\text{–}Me\text{–}Al(C_6F_5)_3]^-$, another metallocene adduct. For Group IV transition metals, such ion pairs have not been observed. For tantalocene, such ion pairs were characterized by X-ray crystallography [7].

In their theoretical work, Eilertsen et al. [8] suggested the double activation mechanism for the formation of active ion pairs in the MAO-containing systems.

The purpose of this theoretical work is to understand the capacity of the aluminum-containing compounds to activate metallocenes. We accept the double activation mechanism and consider $Al(C_6F_5)_3$ as the model cocatalyst. Our initial work in this field [9] dealt with Cp* zirconocenes (Cp* = $\eta^5\text{-}C_5H_5$, $\eta^5\text{-}C_5Me_5$) as transition-metal components. Later, we turned to propylene polymerization catalysts based on *ansa*-CpFlu derivatives of Zr and Hf with $Me_2C <$ and $Ph_2C <$ bridges and with substituted or unsubstituted Cp and Flu moieties. In the framework of the double activation mechanism, we arranged the CpFlu zirconocenes in order of increasing numbers of active sites. Furthermore, we established an order of increasing activities per zirconium site for propylene polymerization.

[1] The article was translated by the authors.

Table 1. Selected geometry parameters of the (η^5-$C_5H_4CR_2$-η^5-$C_{13}H_8$)MCl_2 (M = Zr, Hf; R = Ph, Me) complexes from X-ray crystallographic data [16, 18] and from DFT calculations

Entry	Bond	Bond length, Å					
		X-ray diffraction data [16, 18]			calculated data		
		Hf	Zr	Δ(Zr–Hf)	Hf	Zr	Δ(Zr–Hf)
1	M–Cl	2.403	2.424	0.03	2.41	2.44	0.03
		(2.391/2.394)	(2.422/2.425)	(0.03/0.03)	(2.41)	(2.44)	(0.03)
2	M–C(1)	2.410	2.417	0.01	2.44	2.46	0.02
		(2.40)	(2.401)	(0.00)	(2.44)	(2.45)	(0.01)
3	M–C(2)	2.511	2.513	0.02	2.55	2.58	0.03
		(2.49/2.57)	(2.501/2.528)	(0.01/–0.04)	(2.57)	(2.60)	(0.03)
4	M–C(7)	2.670	2.680	0.01	2.73	2.76	0.03
		(2.64)	(2.651/2.655)	(0.01/0.02)	(2.73)	(2.75)	(0.02)
5	M–C(27)	2.440	2.452	0.01	2.46	2.48	0.02
		(2.46)	(2.436)	(–0.02)	(2.46)	(2.47)	(0.01)
6	M–C(28)	2.439	2.450	0.02	2.46	2.48	0.02
		(2.41/2.44)	(2.444/2.452)	(0.03/0.01)	(2.47)	(2.48)	(0.01)
7	M–C(29)	2.505	2.523	0.02	2.53	2.55	0.02
		(2.50/2.51)	(2.519/2.528)	(0.02/0.02)	(2.54)	(2.56)	(0.02)
		Angle, deg					
	Bond angle	Hf	Zr	Δ(Zr–Hf)	Hf	Zr	Δ(Zr–Hf)
8	Cl–M–Cl	95.6	95.9	0.3	97.8	99.0	1.2
		(97.5)	(98.2)	(0.7)	(98.8)	(100.3)	(1.5)

Atomic numbering in these complexes is the same as in [16]:

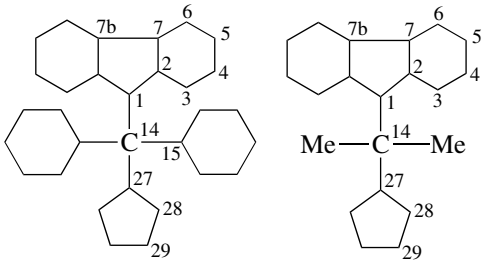

The bond lengths for R = Me are in parentheses. Because both (η^5-$C_5H_4CMe_2$-η^5-$C_{13}H_8$)MCl_2 complexes are not symmetrical in crystals, we list two values of the bond length in one cell (entries 1, 3, 4, 6, and 7).

METHODS

Computational Details

All calculations were carried out by the DFT method using the original program Priroda [10]. The generalized gradient approximation (GGA) for the PBE exchange-correlation functional [11] and an orbital basis set of contracted Gaussian-type three-exponential functions were employed. Twenty-eight core electrons of Zr, 60 core electrons of Hf, 10 core electrons of Cl, Al and 2 core electrons of C and F were described in terms of effective core potentials [12–14]. This approach takes into account relativistic effects. They are of particular significance for Hf-containing compounds. Geometry was optimized without imposing any symmetry constraints.

It was shown that the approximation described above correctly reproduces the geometrical parameters of the adducts formed by Cp* zirconocenes and B-containing Lewis acid sites [15].

In Table 1, we compare the experimental and calculated geometries of Zr- and Hf-containing CpFlu metallocenes, using the (η^5-$C_5H_4CR_2$-η^5-$C_{13}H_8$)MCl_2 (R = Me, Ph) compounds as examples. Their optimized structures are shown in Fig. 1. The experimental geometrical parameters were taken from [16–18]. For these metallocenes, the calculated geometrical parameters are in good agreement with experimental data (Table 1). However, in certain cases (entries 2–7), the calculated M–C distances are longer than experimental ones.

It is interesting to compare the reactivities of Zr- and Hf-containing complexes with the same ligands. Note that the calculated difference between the Zr–C and Hf–C bond lengths (parameter Δ(Zr–Hf)) is in a good agreement with experimental data (Table 1, entries 2–7). Any Z–C bond is ~0.01–0.02 Å longer than the corresponding Hf–C bond.

The discrepancies between the calculated structure parameters and the same parameters derived from X-ray diffraction data can be due to the fact that the molecular geometry in the crystal is distorted as compared to the gas-phase geometry. According to X-ray crystallographic data [18], C–C bond lengths in the fluorenyl moiety of $(\eta^5\text{-}C_5H_4CPh_2\text{-}\eta^5\text{-}C_{13}H_8)MCl_2$ are essentially different both in the Zr- and Hf-containing compounds. However, this is not the case for the calculated bond lengths. Furthermore, the complexes $(\eta^5\text{-}C_5H_4CR_2\text{-}\eta^5\text{-}C_{13}H_8)MCl_2$ (both with Zr and with Hf) are not symmetrical in their crystals [17], unlike the R = Ph compounds[18]. The calculated structures of all of these complexes, both with R = Me and with R = Ph, have a symmetry plane.

Transition State Optimization

The initial search for transition states (TS's) was carried out for a "cation" model of the catalyst. TS structures for the cation model were obtained by means of complete geometry optimization after calculating the energy of the system as a function of the interatomic distances in the forming C–C bonds. The geometries characterized by the highest energies were used as initial approximations for further computations aimed at complete TS optimization. The type of stationary points was determined by calculating the second derivatives of energy with respect to the coordinates and by vibrational spectrum analysis. Among the rather wide variety of optimized transition states, we found the lowest energy one. This structure was used to construct the initial structure for the TS containing the counterion $[(C_6F_5)_3Al\text{–}Me\text{–}Al(C_6F_5)_3]^-$. As will be demonstrated below, in all cases, the counterions are separated by a long distance. Therefore, the presence of an anion does not disturb the structure of the cation moiety characteristic of the pure cation model. This allowed us to minimize the run time in TS optimization by using the following approach. The C–C distance in the forming bond was fixed at the value obtained within the framework of the cation model, whereas the other geometrical parameters were allowed to vary in the course of geometry optimization.

Note that the geometry and energy of the system obtained by this method were practically the same as the values calculated for the real TS determined by means of complete geometry optimization for the system containing the counterion. The computation time was thus shortened by a factor of ~10.

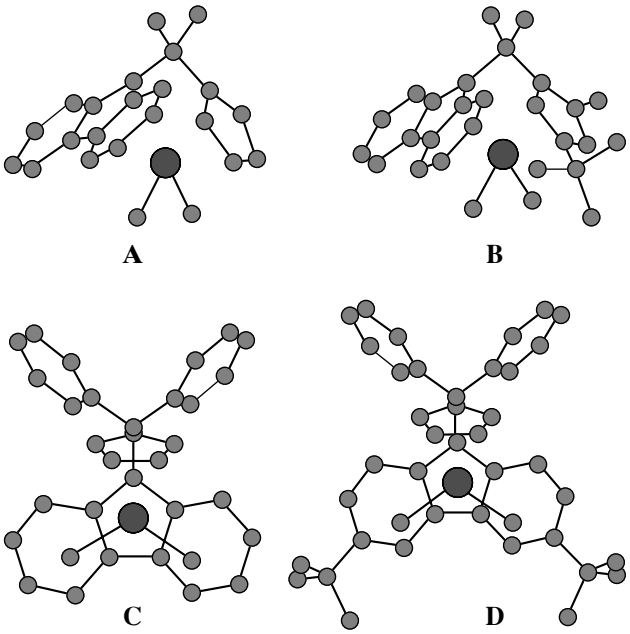

Fig. 1. Structures of the catalyst precursors (M = Zr, Hf; the hydrogen atoms are not shown): (**A**) $(\eta^5\text{-}C_5H_4CMe_2\text{-}\eta^5\text{-}C_{13}H_8)MCl_2$, (**B**) $(\eta^5\text{-}3\text{-}tert\text{-}Bu\text{-}5\text{-}Me\text{-}C_5H_2CMe_2\text{-}\eta^5\text{-}C_{13}H_8)MCl_2$, (**C**) $(\eta^5\text{-}C_5H_4CPh_2\text{-}\eta^5\text{-}C_{13}H_8)MCl_2$, and (**D**) $(\eta^5\text{-}C_5H_4CPh_2\text{-}\eta^5\text{-}3,6\text{-di-}tert\text{-}Bu\text{–}C_{13}H_6)MCl_2$.

RESULTS AND DISCUSSION

The most significant distinction between $Al(C_6F_5)_3$ and $B(C_6F_5)_3$ is the ability of $Al(C_6F_5)_3$ to form Al–C–Al bridges. For this reason, after the methylation of the metallocene during the formation of a catalytic site, the following symmetrical anion may be formed:

$$[(C_6F_5)_3Al\text{–}CH_3]^- + Al(C_6F_5)_3 \longrightarrow [(C_6F_5)_3Al\text{–}CH_3\text{–}Al(C_6F_5)]^-. \quad \text{(I)}$$

The optimized structure of this counterion is shown in Fig. 2. Its formation (reaction (I)) is thermodynamically favorable: the energy of the system decreases by 30.2 kcal/mol.

Cp-based Zirconocenes: Calculation of Energy and Geometrical Parameters

As was mentioned above, excess $Al(C_6F_5)_3$ is required for polymerization to occur. The excess aluminum ensures the efficient formation of metallocene adducts with two $Al(C_6F_5)_3$ molecules (ion pair (IP) and "double adduct" (DA)). The formation of such adducts is illustrated by the example of Cp_2ZrMe_2 in Scheme 1. Their optimized structures are presented in Fig. 3.

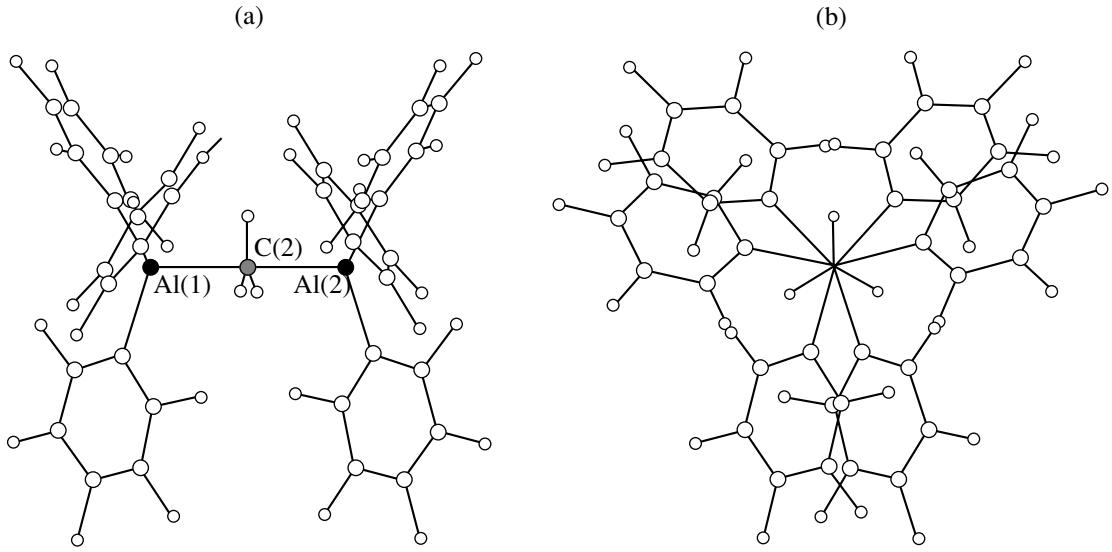

Fig. 2. Structure of the $[(C_6F_5)_3Al–Me–Al(C_6F_5)_3]^-$ anion: (a) top view and (b) side view.

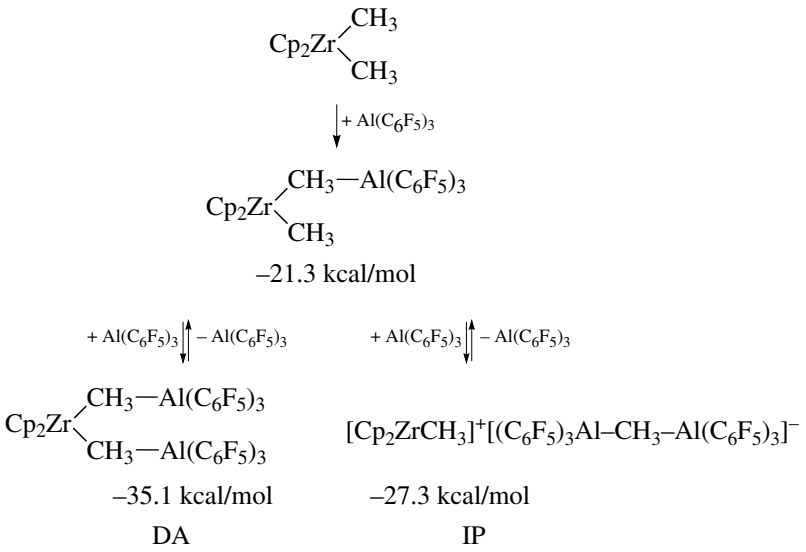

Scheme 1.

The adduct IP (Fig. 3a) includes a $[(C_6F_5)_3Al–CH_3–Al(C_6F_5)]^-$ counterion. It is important that the Me group in IP is completely transferred to Al. Since a vacancy for olefin coordination is also present in IP, it can be considered an active site of polymerization. This structure is described in detail elsewhere [9]. The energy of the IP structure is 27.3 kcal/mol lower than the sum of the energies of the initial reagents.

The double adduct that appears in the scheme (a zirconocene complex with unsubstituted Cp rings and two μ-Me groups (Fig. 3b)) has a lower energy than IP. Its formation decreases the energy of the system by 35.1 kcal/mol relative to the noninteracting reagents. Unlike IP, DA is not separated into a cationic and anionic parts. A coordination vacancy required for monomer binding is also absent in DA. Therefore, DA cannot be a catalytic site.

The energy difference between DA and IP can be viewed as a measure of the active site (IP) content of the equilibrium mixture of IP and inactive compounds (DA).

To simulate the polymerization reaction, the methyl groups in IP and DA were replaced by ethyl groups. The ethyl group can be considered as an adequate model of the growing polymer chain [5], since it makes it possible to take into account the α- and β-agostic interactions, which are important for polymerization.

The replacement of one of the methyl groups in the metallocene with ethyl allows several IP and DA isomers to exist (as is illustrated in the diagram by the example of a metallocene with unsubstituted Cp rings). These isomers differ by the rotation angle of the ethyl group and by the presence (or absence) of agostic bonds. The energy difference between the isomers for each type of IP and DA is a few kilocalories. The energy difference between the most stable isomers of IP and DA was chosen as the criterion of catalyst activity. For example, for the Cp-ring zirconocenes, the most stable DA is the backside β-agostic isomer and the most stable IP is the frontal one.

The energy differences between DA and IP at the stages of active site formation and polymer chain growth (ΔE(Me) and ΔE(Et), respectively) are listed in Table 2. As is clear from Table 2, the growing polymer chain decreases the energy difference between IP and DA. Therefore, the introduction of the monomer into these systems shifts the equilibrium between IP and DA towards the formation of active sites (IPs). Furthermore, the introduction of donor substituents into the Cp ring also leads to a decrease in ΔE(Me) and ΔE(Et). For example, in the case of pentamethyl-substituted zirconocene and the Et ligand (as a model of the polymer chain), IP is more stable than DA (Table 2) and, therefore, the system is dominated by active IP species.

Below, we demonstrate how the above statements can be used to estimate the activity of Zr and Hf catalysts for propylene polymerization (Fig. 1). Computations were performed for catalyst precursors with ligands containing a Cp or Flu moiety and with a $CMe_2<$ or $CPh_2<$ bridge (**A**, **C**). Flu-di-*tert*-Bu-substituted (**D**) and Cp-Me,*tert*-Bu-substituted (**B**) catalyst precursors with Me- (**B**) and Ph-substituted (**D**) methylene bridges were also considered.

CpFlu Metallocene Complexes (Cp–CR_2–Flu)M(Me–Al(C_6F_5)$_3$)(X–Al(C_6F_5)$_3$) and the Corresponding Ion Pairs (Cp–CR_2–Flu)MX]$^+$[(C_6F_5)$_3$AlMe–Al(C_6F_5)$_3$]$^-$ with and without Substituents in the Flu or Cp Moiety of the Ligand (M = Zr, Hf; R = Me, Ph; X = Me, Et): Calculation of Geometry and Energy Parameters

Change in the number of active sites. For all of the systems based on the precursors **A**–**D** (Fig. 1), the catalytically inactive form DA has a lower energy than the active form IP. The lower the value of ΔE, the higher the number of active sites in the equilibrium mixture of the two products.

As in the above simpler systems (see the above diagram), there can be several isomers differing in the conformation of the ethyl group and in the orientation of this group relative to the "core" [(η^5-$C_5H_4CR_2$-η^5-$C_{13}H_8$)M]: (1) backside, nonagostic; (2) frontal, nonagostic; (3) backside, β-agostic; and (4) frontal, β-agostic.

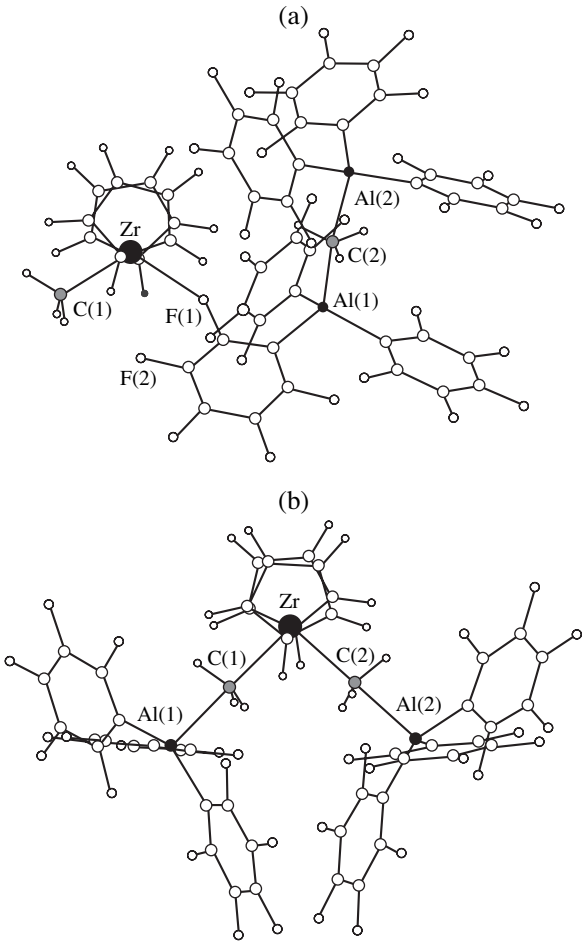

Fig. 3. (a) IPs and (b) DAs in the system Cp_2ZrMe_2 + Al(C_6F_5)$_3$.

Since there are several isomers for each IP and DA, it again seems reasonable to compare the energies of the most stable isomers. These isomers are nonagostic for IP and agostic for DA.

One can see from Table 3 that the number of active sites is larger during polymerization than in the absence of a monomer, as in the case of the Cp*-based metallocenes.

Table 2. Energy difference between DA and IP for the Cp* systems with Al(C_6F_5)$_3$ at the stages of active site formation (ΔE(Me)) and polymer chain growth (ΔE(Et))

Zirconocene	ΔE, kcal/mol	
	X = Me	X = Et
Cp_2ZrMeX	7.8	3.4
$(CpMe_5)_2ZrMeX$	5.6	–4.9

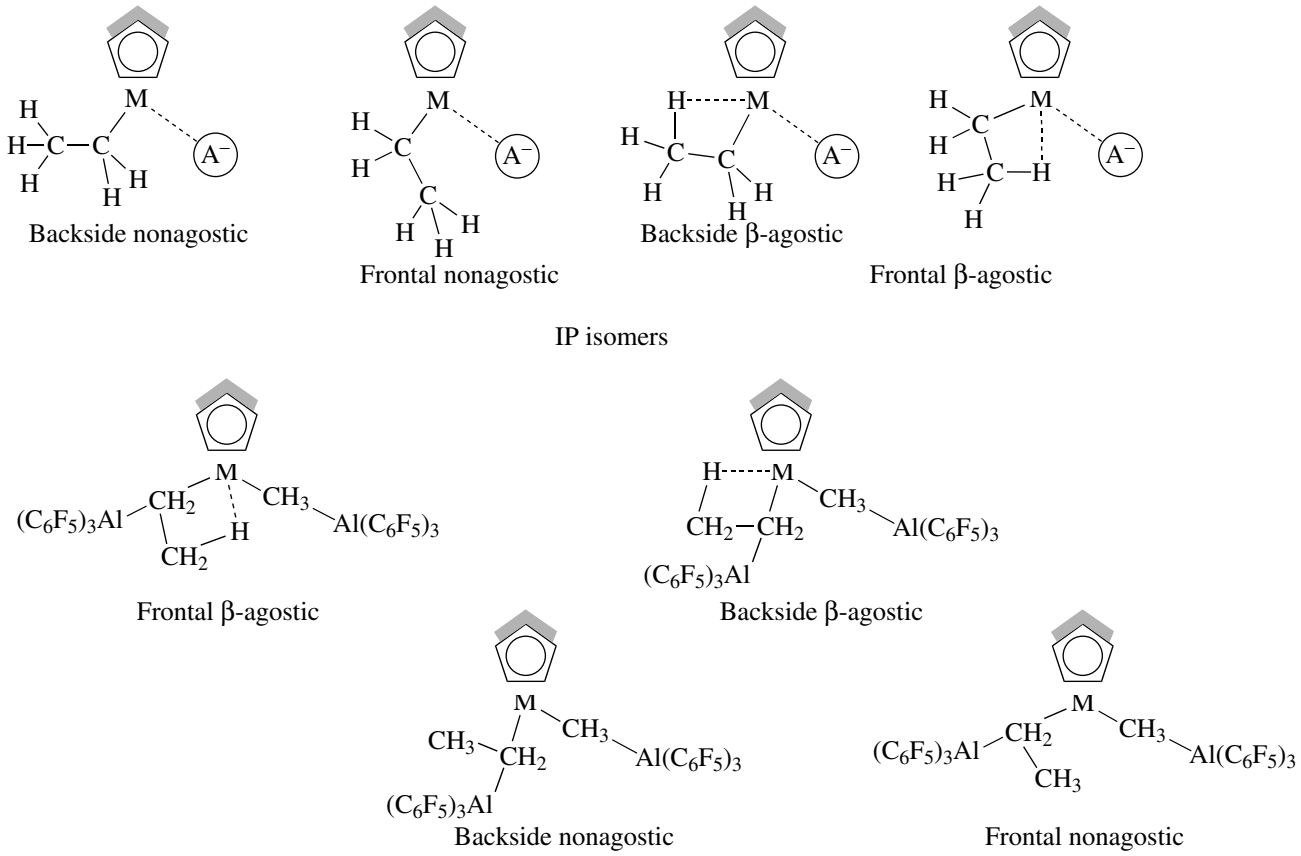

Scheme 2.

The number of active sites must be larger for the $CPh_2<$-bridged catalyst precursors (**C**) with unsubstituted CP and Flu moieties than for the corresponding $Me_2C<$-bridged ones (**A**). The introduction of two *tert*-Bu groups into the Flu moiety of the ligand of the $Ph_2C<$-bridged metallocenes (**D**) must cause an increase in the number of active sites, whereas the introduction of substituents into the Cp ring (**B**) must exert an opposite effect.

Table 3 demonstrates that the zirconocene-based systems have more active sites than the hafnocene-based systems, except for the $Ph_2C<$-bridged metallocenes containing two *tert*-Bu groups in the Flu moiety of the ligand (**D**). In this case, the number of active sites in polymerizable systems is similar for Zr and Hf. Thus, the lower catalytic activity of the hafnocene-based system as compared to the zirconocene-based systems can be due to the fact that the former have a smaller number of active sites.

TS energies for polypropylene chain growth. The interaction between an active site and the monomer is described by the following reaction:

$$\{L\}MR^+ A^- + C_3H_6$$
$$\xrightarrow{1} \{L\}M(C_3H_6)R^+A^- \qquad \text{(II)}$$
$$\xrightarrow{2} (L)MC_2H_3(CH_3)R^+A^-.$$

To determine the reactivity of the catalytic site interacting with C_3H_6, we calculated the TS energy (E(TS)) for the second stage of reaction (II) (chain growth) relative to the sum of the energies of $\{L\}MR^+A^-$ and C_3H_6. This parameter takes into account both the energy barrier in stage 2 and the increase in energy due to the charge separation in stage 1. These calculations were performed for zirconocenes (Table 3).

According to our estimates, the binding of a substrate molecule is accompanied by a decrease in entropy ($T\Delta S \approx -10$ kcal/mol at $T = 298$ K). Therefore, the change in free energy for TS formation, G(TS), will be positive (see the Gibbs energy diagram for reaction (II)). This means that the free energies of the TS's are higher than the sum of the free energies of the

Table 3. Energy differences (ΔE) between IPs and the corresponding DAs (M = Zr, Hf) and the energy of transition state (E(TS)) relative to the sum of the energies of the noninteracting propylene molecules and initial Zr-containing IPs

Catalyst precursor	ΔE, kcal/mol				E(TS), kcal/mol
	X = Me		X = Et		
	M = Hf	M = Zr	M = Hf	M = Zr	M = Zr
A	12.4	9.6	5.7	4.4	–5.2
B	12.5	9.7	7.7	3.5	–5.6
C	11.2	8.2	4.6	5.2	–4.8
D	7.8	5.5	1.0	1.1	–2.8

nonreacting reagents and correspond to saddle points in the reaction path.

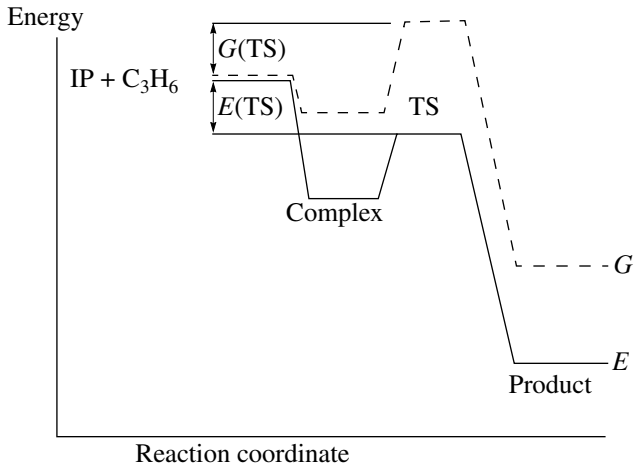

As is specified above, the initial search for TS's was carried out for a cation model of the catalyst. The *iso*-Bu group was taken to be the model of the growing polymer chain—the most realistic choice in this case. We considered all possible α- and β-agostic TS structures and all possible propylene orientations in the coordination sphere of Zr.

The TS energy increases in the order **B < A < C < D** (Table 3), implying a decrease in the reactivity of a single Zr-containing site. Therefore, for all of the zirconocenes presented in Table 3 ($Al(C_6F_5)_3$ is the cocatalyst), an increase in the number of catalytic sites (IPs) is accompanied by an increase in the energy barrier of the reaction, retarding the reaction at each individual catalytic site. We assume that this effect is due to IP stabilization relative to the structures without charge separation ($\{L\}M(R)Me + Al(C_6F_5)_3$, DA, etc.) or the structures with weakly interacting components (e.g., the complex $\{L\}M(C_3H_6)R^+A^-$ and the TS corresponding to its conversion into the product $\{L\}MC_2H_3(CH_3)R^+A^-$ in reaction (II)). This stabilization is determined by the interaction between $\{L\}M(C_3H_6)R^+$ and A^-.

If the polymerization rate were controlled solely by E(TS), one would expect that this rate decreases in the above order. However, a different situation may be observed, since, as mentioned above, the energy difference between the DA and IP also decreases in this order (Table 3). Therefore, an increase in the energy barrier, which slows down the reaction at each individual catalytic site, will be accompanied by a buildup of active catalytic sites (IPs). The competition between these factors (the energy barrier and the number of active sites) will determine the changes in the polymerization rate in passing from compound **A** to compound **D**. Furthermore, variations in polymerization conditions (such as temperature) can also influence the relative activities of the catalytic systems.

Thus, a method has been developed for the determination of a relative amount of catalytic sites and of the reactivity of an individual site in the framework of the double activation mechanism. This approach is based on the calculation of the energy parameters $\Delta E = E(IP) - E(DA)$ and E(TS).

Extending this approach to the MAO-containing systems provides an explanation for the large Al/M ratio required for catalyst activation. Indeed, two Lewis acid sites in an aluminoxane globule must be separated by ~4.3 Å and must be oriented so that the Al atoms face each other. The larger the ratio between Al and M, the higher the probability of this configuration.

ACKNOWLEDGMENTS

This work was supported by the Russian Foundation for Basic Research (project nos. 04-03-33042 and 05-03-33114) and Atofina Research S.A.

REFERENCES

1. Yang, X., Stern, C.L., and Marks, T.J., *J. Am. Chem. Soc.*, 1991, vol. 113, p. 3623.
2. Eur. Pat. Appl. EP 0427697, 1991.
3. Lanza, G., Fragala, I.L., and Marks, T.J., *J. Am. Chem. Soc.*, 2000, vol. 122, p. 12 764.
4. Chan, M.S.W. and Ziegler, T., *Organometallics*, 2000, vol. 19, p. 5182.
5. Nifant'ev, I.E., Ustynyuk, L.Yu., and Laikov, D.N., *Organometallics*, 2001, vol. 20, p. 5375.

6. Chen, E.Y.-X., Kruper, W.J., Roof, G., Wilson, D.R., *J. Am. Chem. Soc.*, 2001, vol. 123, p. 745.
7. Chen, E.Y.-X. and Abboud, K.A., *Organometallics*, 2000, vol. 19, p. 5541.
8. Eilertsen, J.L., Stivneng, J.A., Ystenes, M., and Rytter, E., *Future Technology for Polyolefin and Olefin Polymerization Catalysis*, Tokyo: Technology and Education, 2002, p. 111.
9. Ustynyuk, L.Yu. and Fushman, E.A., *Zh. Fiz. Khim.*, 2004, vol. 78, no. 6, p. 1080.
10. Laikov, D.N., *Chem. Phys. Lett.*, 1997, vol. 281, p. 151.
11. Perdew, J.P., Burke, K., and Ernzerhof, M., *Phys. Rev. Lett.*, 1996, vol. 77, p. 3865.
12. Stevens, W.J., Basch, H., and Krauss, M., *J. Chem. Phys.*, 1984, vol. 81, p. 6026.
13. Stevens, W.J., Basch, H., Krauss, M., and Jasien, P., *Can. J. Chem.*, 1992, vol. 70, p. 612.
14. Cundari, T.R. and Stevens, W.J., *J. Chem. Phys.*, 1993, vol. 98, p. 5555.
15. Nifant'ev, I.E. and Ustynyuk, L.Yu., *Zh. Fiz. Khim.*, 2002, vol. 76, no. 8, p. 1453.
16. Razavi, A. and Atwood, J.L., *J. Organomet. Chem.*, 1993, vol. 459, p. 117.
17. Razavi, A., Peters, L., and Nafpliotis, L., *J. Mol. Catal. A: Chem.*, 1997, vol. 115, p. 129.
18. *Cambridge Structural Database.*